# *The importance of wetlands in the energy balance of an agricultural landscape*

**Hanna Huryna, Jakub Brom & Jan Pokorny**

**Wetlands Ecology and Management**

ISSN 0923-4861

Wetlands Ecol Manage
DOI 10.1007/s11273-013-9334-2

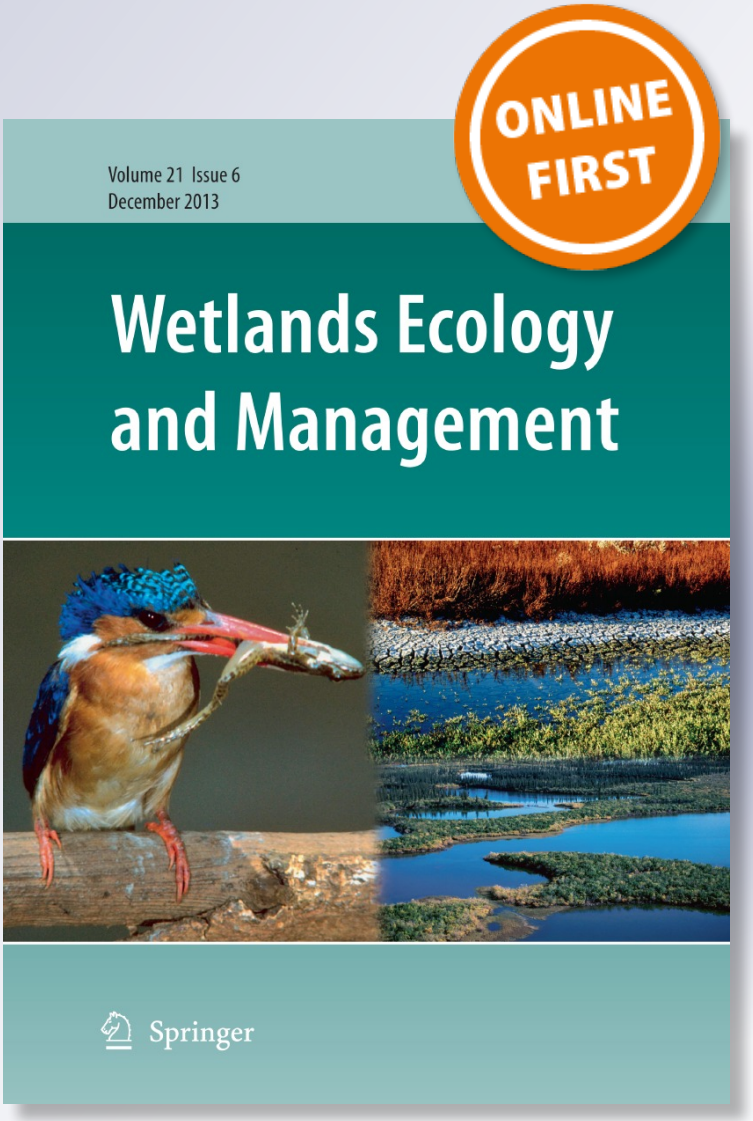


Springer

Wetlands Ecol Manage
DOI 10.1007/s11273-013-9334-2

ORIGINAL PAPER

# The importance of wetlands in the energy balance of an agricultural landscape

**Hanna Huryna · Jakub Brom · Jan Pokorny**

Received: 21 January 2013 / Accepted: 10 December 2013


**Abstract** Energy fluxes, including net radiation, latent heat flux and sensible heat flux were determined on clear days during the vegetative period in four types of land cover: wet meadow, pasture, arable field, and an artificial concrete surface. The average net radiation ranged between 123 W $m^{-2}$ at the concrete surface and 164 W $m^{-2}$ at the wet meadow. The mean maximum daytime latent heat ranged between 500 and 600 W $m^{-2}$, which corresponds to an evapotranspiration rate of about 0.2 g $m^{-2}$ $s^{-1}$ under the prevailing conditions of the wet meadow. The results demonstrated that the wet meadow dissipated about 30 % more energy through evapotranspiration than the field or the pasture, and up to 70 % more energy than the concrete surface. The evaporative fraction indicated that more than 100 % of the energy released by the wet meadow was dissipated through evapotranspiration; this was attributed to local heat advection. Wetland evapotranspiration thus contributes significantly to the cooling of agricultural landscapes; the energy released can reach several 100 MW $km^{-2}$. Wetland evapotranspiration has a double 'air conditioning' effect through which it equalises temperature differences: (1) surplus solar energy is bound into water vapour as latent heat; (2) The vapour moves towards cooler portions of the atmosphere where the energy is released. The air-conditioning effect of wetlands plays an important role in mitigating local climate extremes; this ecosystem service tends to be disregarded in relation to other better-known wetland functions such as nutrient retention and provision of high biodiversity.

**Keywords** Heat balance · Bowen ratio · Evapotranspiration · Evaporative fraction · Heat advection · Local climate

H. Huryna
Faculty of Science, University of South Bohemia, Branisovska 31a, 370 05 Ceske Budejovice, Czech Republic

H. Huryna (✉) · J. Pokorny
ENKI, o.p.s, Dukelská 145, 379 01 Třeboň, Czech Republic
e-mail: huryna@nh.cas.cz

J. Pokorny
e-mail: pokorny@enki.cz

J. Brom
Faculty of Agriculture, University of South Bohemia, Studentská 13, 370 05 Ceske Budejovice, Czech Republic
e-mail: jbrom@zf.jcu.cz

## Introduction

Human activities in rural areas have dramatically altered the nitrogen and water cycles over the last century. Wetland drainage and the widespread use of fertilisers have increased the amount of nutrients present in groundwater as well as in surface waters (Ripl 2003). The nutrient retention efficiency of

Published online: 24 December 2013

natural and constructed wetlands used for agricultural purposes has been documented (Craft 1996; Fisher and Acreman 2004; Silvan et al. 2004; Hussain and Badola 2008; Powers et al. 2012). Wetlands are more efficient than other land cover types in performing these 'services', thanks to their ability to retain nutrients, stabilise nutrient cycles and enhance biodiversity within the landscape (Kao et al. 2003). In this study, we show that, in addition to these ecological functions, wetlands can strongly influence local and regional microclimates through evapotranspiration; an important process controlled by the interaction of several environmental and biological factors (Blanken et al. 1997; Wilson and Baldocchi 2000).

Solar energy warms the Earth at an average of 15 °C or 288 K. The amount of direct solar irradiance at the top of Earth's atmosphere fluctuates through each calendar year from 1,412 W $m^{-2}$ in early January to 1,321 W $m^{-2}$ in early July, because of the Earth's varying distance from the Sun on the elliptic trajectory (Geiger et al. 2003; Kopp et al. 2005). The amount of solar energy received at the earth surface varies by latitude and according to daily and seasonal pulses. The mean dissipation of solar energy in different months is shown on the NASA SSE web-site (http://eosweb.larc.nasa.gov/sse). The amount of energy received as incoming solar radiation within the temperate zone (Central Europe, Czech Republic) every year is about 1,150 kWh $m^{-2}$, with slight variations depending on the latitude. The annual average in the centre-North of the USA reaches up to 1,365 kWh $m^{-2}$, while in Florida (USA), it is 1,745 kWh $m^{-2}$. The maximum irradiance (instantaneous flux) commonly lies between 800 and 1,000 W $m^{-2}$ in the tropics and subtropics, which is similar to the irradiance occurring in temperate zones during the growing season. The amount of incoming energy differs significantly depending upon weather conditions. The difference between the maximum incoming solar radiation on a clear day can be an order of magnitude higher than the incoming radiation on an overcast day (Huryna and Pokorný 2010).

The largest part of the energy received during the growing season in most sites is converted into the latent heat of evapotranspiration. Functional properties and processes, such as soil moisture content, vegetative production and nutrient, and water cycling, are all influenced by evapotranspiration. The conversion of incoming energy into latent heat and sensible heat fluxes has a significant impact on local climate, as this process drives exchanges of energy and mass between the surface of continents and the atmosphere (Pielke et al. 1998). Makarieva and Gorshkov (2007) and Makarieva et al. (2013) described the fundamental role of forest evapotranspiration in the transport of water vapour from seas into continents and showed that the latent heat flux of evapotranspiration represents a process that directly links the energy and the water budgets of the landscape. The balance between the two plays a fundamental role in the cycling of water within terrestrial ecosystems and thus influences local climate patterns. Evapotranspiration is considered a driving force of landscape sustainability (Ripl 2003; Eiseltová et al. 2012). The water cycle is continuously driven by the Sun's irradiation, and it plays a key role in the dissipation of solar energy and in the cycling of matter. Ecosystems, like other living systems, are dissipative structures in terms of non-equilibrium thermodynamic (Capra 1996; Schneider and Sagan 2005); they tend to release heat and to use solar energy for self-organisation.

When the Earth's surface has no plant cover, or when there is not enough water for evapotranspiration, solar energy heats the land surface, which then transfers it to the air immediately above by generating sensible heat. Under high irradiance barren surfaces, such as agricultural fields after harvesting and urban tar-sealed surfaces become landscape 'hot spots', generating strong turbulence in the atmosphere above them (Kedziora 2004; Schneider and Sagan 2005; Kravčík et al. 2008).

The energy balance of a surface well supplied with water is presented in Fig. 1. The net radiation is the balance between incoming and outgoing short- and longwave radiations. In plants' stands, the net radiation is largely dissipated through the evaporation of water from plants and soil, partly converted into sensible heat and partly transported into ground as the conductive soil heat flux. A minor part of net radiation is accumulated in biomass through photosynthesis.

The rate of evapotranspiration is determined by solar energy, air humidity, water availability, atmospheric pressure, as well as by relevant biological factors. The most important biological factor is the physiology of the plant species that cover the landscape surface, and their stage of development (Ryszkowski and Kedziora 1995).

A number of recent studies have focused on the dissipation of energy fluxes over several years (e.g.

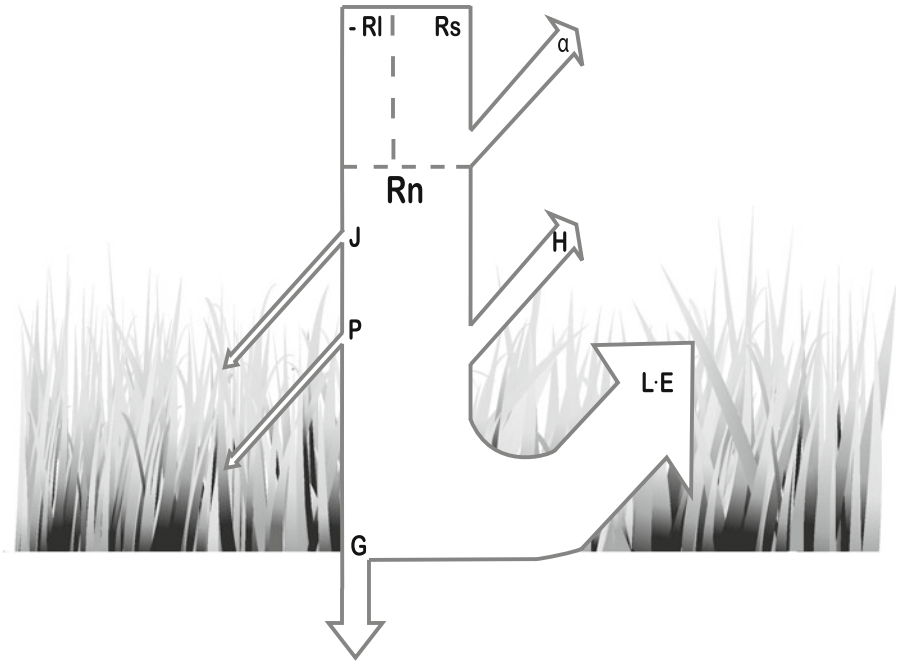


**Fig. 1** Dissipation of solar energy in a plant stand well supplied with water. $R_s$ shortwave radiation, $R_l$ longwave radiation, $\alpha$ albedo, $R_n$ net radiation, $H$ sensible heat, $LE$ latent heat of evapotranspiration, $G$ ground diffusion, $J$ accumulation of heat in biomass, $P$ energy consumption by photosynthesis

von Randow et al. 2004; Burba and Verma 2005; Liu et al. 2009); within a single year (Gu et al. 2005; Blanken et al. 2009); throughout the growing season (Ryszkowski and Kedziora 1987; Olejnik 1988; Wever et al. 2002; Kurc and Small 2004) and over several days (Olejnik et al. 2001; Pivec 2002; Eulenstein et al. 2005; Brom and Pokorný 2009; Rejšková et al. 2010). The seasonal heat balance of riparian buffer strips, meadows, agricultural fields (rape seed, beet and wheat) and bare soil was evaluated by Ryszkowski and Kedziora (1987) in the Turew region of Poland. They found that the net radiation ranged from 1.84 kWh $m^{-2}$ $d^{-1}$ (within the meadow) to 2.14 kWh $m^{-2}$ $d^{-1}$ (within riparian buffers) because of the differences in albedo. The energy consumed in evapotranspiration during the vegetative season ranged from 1.07 kWh $m^{-2}$ $d^{-1}$ for the bare soil to 1.88 kWh $m^{-2}$ $d^{-1}$ for the riparian buffer strips.

The roles of plants in the sequestration of carbon dioxide and in maintaining the oxygen concentration of the atmosphere are generally well understood. The photosynthetic exchange of $CO_2$ and $O_2$ is accompanied by a large release of transpired water: one molecule of oxygen is released for each molecule of utilised carbon dioxide, while several 100 molecules of water are evaporated (Schulze et al. 2002; You et al. 2009; Pokorný et al. 2010). It has been known from the 1950s that wetlands vegetation well supplied with water are able to convert several 100s (W $m^{-2}$) of solar energy into evapotranspiration (Penman 1948; Monteith 1981). This direct effect of wetlands on climate has been overlooked, however, in the discussion on the impact of humans on climate changes. The indirect effect of wetlands on climate, i.e. sink/source of greenhouse gases (GHG), has been intensively studied and presented to decision makers and to the public (IPCC 2007). According to IPCC (2007), radiative forcing is the net change in the energy balance of the Earth system (stratospherically adjusted radiative flux change evaluated at the tropopause) in response to an increase in GHG in the atmosphere. It is equal to 1–3 W $m^{-2}$ for the period from 1750 until present time. In the next 10 years, the radiative forcing is expected to increase by 0.2 W $m^{-2}$.

The aim of our study is to show the direct effect of wetlands and their vegetation cover upon regional climate through the dissipation of the incoming solar radiation and its relation to the water cycle. Our study is based upon time-intensive quantitative measurements

of dissipated solar energy, conducted over a whole year, comparing a wet meadow, a wet pasture, an open arable field and a concrete surface.

## Methods and site description

Throughout the text, we will use the following terms, according to Parker (2002):

- 'Energy flux' is a vector quantity component of which perpendicular to any surface equals the energy transported across that surface by some medium per unit area per unit time.
- 'Energy dissipation' is any loss of energy, generally by conversion into heat (as well as into latent heat); its quantification consists in establishing the rate at which this loss occurs.
- 'Heat balance' is the equilibrium which exists on average between the radiation received by the earth and atmosphere from the sun and that emitted by the earth and atmosphere.

The study was undertaken in an alluvial lowland within the Třeboň Biosphere Reserve in southern Bohemia, (TBBR) (48°49′ to 49°20′N; 14°39′ to 15°00′E) near the Czech–Austrian border. The flat bottom of the basin is at 410–470 m a.s.l., with an undulating margin reaching 550 m. The Třeboň Basin, the southernmost portion of the large Vltava catchment, belongs to a moderately warm region of the Central European temperate zone, with an annual mean temperature of 8 °C and a mean annual precipitation of 650 mm. The TBBR (700 $km^2$ in total), has about 500 fishponds cumulative surface of which reaches 7,500 ha. Forestry, agriculture and fisheries have always been the main activities (Květ et al. 2002).

Four experimental sites were selected within a distance of between 2 and 4 km from each other:

(1) A wet meadow (ca. 500 ha) within the Rožmberk fishpond (480 ha) catchment. Dominant species were high sedges *(Carex acuta, Carex vesicaria), Calamagrostis canescens, Phalaris arundinacea, Urtica dioica*. The area surrounding the meteorological station is not managed; tall vegetation is regularly cut only in the close vicinity of the meteorological station. The drier parts of the wet meadow are mown once a year. The wet meadow is an epilittoral (upper littoral) of Rožmberk fishpond which is inundated during an exceptionally high water level, mostly in spring or any rainy period. In the flat Třeboň Basin, such an epilottoral inundated area may be even larger than the fishpond area at standard water level.

(2) A pasture with a relatively high groundwater level, characterised by dominant herbs such as *Alopecurus pratensis, Ranunculus repens, Phleum pratense, Dactylis glomerata, Bellis perennis, Poa palustris, Trifolium repens, Taraxacum sect,* and *Veronica chamaedrys*, Ruderalia.

(3) A winter barley field (22 ha).

(4) An artificial concrete surface (400 $m^2$) located within the area of the Wastewater Treatment Plant of the city of Třeboň.

All four sites were exposed at similar angles to the sun rays, as the surface of the TBBR is flat. The dataset, used for the estimation of energy fluxes, evapotranspiration and micrometeorological conditions, was obtained from automatic meteorological stations M4016 placed at each research location. The details of measurement, equipment and sensors' accuracy are summarised in Table 1.

The meteorological data were recorded during a whole year at 10-minute intervals. Complete series of data from the main part of vegetation season, when evapotranspiration rates were high (from 1 May to 31 August 2008), were used for the analysis. The data were arranged into the following three groups according to the amount of total incoming daily shortwave solar irradiance: overcast (0–3,000 Wh $m^{-2}$), cloudy (3,000–6,000 Wh $m^{-2}$) and clear (over 6,000 Wh $m^{-2}$). The numbers of overcast, cloudy and clear days are presented in Table 2. Data collected on clear days were used to estimate the energy balance to evaluate the ability of the different land covers in dissipating solar energy and in dampening temperature extremes.

We estimated energy used for evapotranspiration, vapour pressure deficit, aerodynamic and surface resistance to investigate the specific physical conditions prevailing at the different sites that could have influenced the monitored parameters. Nine days (three in a row) were selected for the analysis—at the beginning, in the middle, and at the end of the study period.

Albedo was computed as a ratio between reflected ($R_{s\uparrow}$) and incoming ($R_{s\downarrow}$) shortwave radiations:

**Table 1** Details of in situ measurements, equipment and sensors' accuracy

| Parameter | Height (m) | Type of sensors/equipment | Range | Accuracy |
|---|---|---|---|---|
| Air temperature | 0.3; 2 | T/RH probes | −20–80 °C | ± 0.3 °C |
| Relative air humidity | 0.3; 2 | T/RH probes | 0–100 % | ± 2 % |
| Surface temperature | 0; −0.1; −0.2 | Pt 100 | −30 to +200 °C | ± 0.15 °C |
| Shortwave radiation | 2 | CM3 pyranometers, Kipp & Zonen, the Netherlands | 310–2,800 nm | ± 5 % |
| Incoming longwave radiation | 2 | CNR1 Net radiometer, Kipp & Zonen, the Netherlands | 5–50 μm | ± 10 % |
| Wind speed and wind direction | 2 | TM-W2 Prague, Czech Republic | | |
| Atmospheric pressure | 2 | PTB 100 A Vaisala sensor, Finland | 800–1,060 mbars | ± 0.3 mbars |
| Soil moisture | −0.05 | Virrib, AMET, Czech Republic | 5–50 % | ± 0.01 $m^3.m^{-3}$ |

**Table 2** Overcast, cloudy and clear days between 1 May and 31 August were used in the assessment

| Ecosystems | Cloudy | Overcast | Clear |
|---|---|---|---|
| Field | 15 | 47 | 61 |
| Wet meadow | 18 | 54 | 51 |
| Concrete surface | 18 | 48 | 57 |
| Pasture | 16 | 51 | 56 |

$$\alpha = \frac{R_{s\uparrow}}{R_{s\downarrow}} \quad (1)$$

Net radiation was computed from the balance between short-wave and long-wave energy, by using the following formula:

$$R_n = R_{s\downarrow} - R_{s\uparrow} + R_{L\downarrow} - R_{L\uparrow} \quad (2)$$

where long-wave radiation emitted by the surface ($R_{L\uparrow}$, W $m^{-2}$) was computed using the following equation (Brutsaert 1982):

$$R_{L\uparrow} = \varepsilon\sigma(T_c + 273.16)^4 \quad (3)$$

where $\varepsilon$ is the emissivity, $\sigma$ is Stefan–Boltzmann constant (W $m^{-2}$ $K^{-4}$) and $T_c$ is the air temperature at canopy height (°C). Emissivity was set 0.98 for all stations. For emissivity values, see Gates (1980).

Net radiation was partitioned into latent (LE), sensible (H) and ground (G) heat fluxes (Penman 1948):

$$R_n = LE + H + G \quad (4)$$

The Bowen ratio, used to estimate the balance between sensible and latent heat fluxes, was expressed in the form (Bowen 1926):

$$\beta = \frac{H}{LE} = \gamma\frac{T_c - T_a}{e_c - e_a}, \quad (5)$$

by approximating the fluxes by means of the temperature and humidity gradient. In the equation above, $\gamma$ is the psychrometric constant (kPa $K^{-1}$), $T_c - T_a$ is the temperature difference between the air temperature at 2 m above the surface and the air temperature at canopy height (0.3 m), $e_c - e_a -$ is the difference between the water vapour pressures (kPa) at these levels.

The water vapour pressure $e$ (kPa) was computed by the formula:

$$e = \frac{RH \cdot e_w}{100} \quad (6)$$

where $RH$ is the relative air humidity, $e_w$ is the saturation pressure of saturated water (kPa) in the air and at the canopy level, respectively.

The values of saturation pressure were obtained using the modified empirical Magnus–Teten's equation (Buck 1996):

$$e_w = 0.61121exp\left(\left(18.678 - \frac{T}{234.5}\right)\left(\frac{T}{257.14 + T}\right)\right) \quad (7)$$

where $T$ represent the temperatures at 2 m above the surface and at canopy level: ($T_a$) and ($T_c$), respectively.

The water vapour pressure deficit (VPD, kPa) was computed for 2 m above the surface level by the formula:

$$VPD = e_w - e_a \quad (8)$$

The ground heat flux was obtained applying Fourier's law of heat conduction using the vertical method (Oke 1987; Monteith and Unsworth 1990):

$$G = k\frac{T_s - T_{0.2}}{z_s - z_{0.2}} \quad (9)$$

where $k$ is the thermal conductivity of soil (W $m^{-1}$ $K^{-1}$); $T_s$ and $T_{0.2}$ are the soil temperatures at depths $z_s$ and $z_{0.2}$, respectively.

Thermal conductivity depends upon soil moisture content, mineral composition, dry soil density, particle composition, particle size distribution and soil temperature (Wierenga et al. 1969). Experimental thermal conductivity values were published by De Vries (1963); Kimball et al. (1976a, b; Asrar and Kanemasu (1983); De Vries and Philip (1986); Gregory et al. (1991); Sikora and Kossowski (1993); Peters-Lidard et al. (1998); and Ochsner et al. (2001).

The ground heat flux at the concrete surface was computed using an empirical equation due to the difficulty of positioning the thermometers within the concrete and isolating them from contact with the air (Brutsaert 1982).

$$G = cR_n \quad (10)$$

where $R_n$ is the net radiation and $c$ is a constant (for bare soil = 0.3).

The latent heat flux was calculated by Bowen (1926):

$$LE = \frac{R_n - G}{1 + \beta} \quad (11)$$

Then, the sensible heat flux was computed on the basis of difference using the energy balance equation:

$$H = R_n = G - LE \quad (12)$$

Fluxes were considered positive when directed downwards and negative when directed upwards in relation to canopy height.

The evapotranspiration rate (ET, g $m^{-2}$ $s^{-1}$) was computed on the basis of the latent heat flux in the following way:

$$ET = \frac{LE}{L_e} \quad (13)$$

where $L_e$ is the latent heat of evaporation (J $g^{-1}$). Daily sums of ET were expressed in mm.

The ratio of the incoming energy fluxes to the net radiation was used for the comparative analysis of the study sites. Furthermore, the evaporative fraction (EF, rel.) was used for assessing the amount of available energy consumed by evaporation (Lhomme and Elguero 1999; Suleiman and Crago 2004; Gentine et al. 2007). EF was computed using the equation:

$$EF = \frac{LE}{R_n - G} \quad (14)$$

A decoupling coefficient ($\Omega$, unitless) was used for assessing the coupling between vegetation and the atmosphere. It was computed using the following equation (Jarvis and McNaughton 1985):

$$\Omega = \frac{LE}{LE_p} = \frac{\Delta + \gamma}{\gamma + 1\left(\frac{r_c}{r_a}\right)} \quad (15)$$

where $LE_p$ is the flux of potential evaporation (W $m^{-2}$), $\Delta$ is the ratio between the saturation water vapour pressure gradient and the temperature gradient (kPa.°$C^{-1}$), $r_c$ is bulk surface resistance (s $m^{-1}$) and $r_a$ is aerodynamic resistance (s $m^{-1}$). According to Jarvis and McNaughton (1985), the decoupling coefficient (factor) describes how closely the saturation deficit at the canopy (or leaf) surface is linked to that of the air outside the canopy boundary layer. It describes the sensitivity of evaporation to stomatal or surface conductance (Jones 1992). The decoupling coefficient is a dimensionless factor that assumes a value comprised between 0 and 1.

Aerodynamic resistance was computed using the Thom equation (Thom 1975):

$$r_a = \frac{\left[ln\left(\frac{z-d}{z_{0m}}\right) - \psi_m(\varsigma)\right]\left[ln\left(\frac{z-d}{z_{0h}}\right) - \psi_h(\varsigma)\right]}{Uk^2} \quad (16)$$

where $z$ is the height measurement of which was taken to describe the physical conditions of the air (m), $d$ is the displacement height (m), $z_{0m}$ and $z_{0h}$ are aerodynamic roughness parameters referring, respectively, to the momentum and to heat transfer (m), $\Psi_m(\varsigma)$ and $\Psi_h(\varsigma)$ are the stability coefficients referring, respectively, to the momentum and to heat transfer (unitless), $\varsigma$ is the Monin–Obukhov stability parameter, $U$ is the wind speed (m $s^{-1}$) and $\kappa$ is the von-Kármán constant (unitless).

The displacement height was computed as given below (Allen et al. 1998):

$$d = \frac{2}{3}h \quad (17)$$

where $h$ is vegetation height. $z_{0m}$ and $z_{0h}$ were computed according to Allen et al. (1998):

$$z_{0m} = 0.123h \tag{18}$$

$$z_{0h} = 0.1z_{0m} \tag{19}$$

Stability parameters $\Psi_m(\varsigma)$ and $\Psi_h(\varsigma)$ were computed for stable ($\varsigma \geq 0$) and unstable or near neutral atmospheric conditions ($\varsigma < 0$) (Foken 2008). Stability parameters for unstable and near neutral atmospheric conditions were computed in the following way (Liu et al. 2007):

$$\Psi_m(\varsigma) = 2ln\left(\frac{1+x}{2}\right) + ln\left(\frac{1+x^2}{2}\right) - 2\arctan(x) + \frac{\pi}{2} \tag{20}$$

$$\Psi_h(\varsigma) = 2\ln\left(\frac{1+x^2}{2}\right) \tag{21}$$

where

$$x = (1 - 16\varsigma)^{0.25} \tag{22}$$

The stability parameters for stable atmospheric conditions (where $\varsigma \geq 0$) were computed according to Beljaars and Holstag (1991):

$$\Psi_m(\varsigma) = -\left[a\varsigma + b\left(\varsigma - \frac{c}{d}\right)\exp(-d\varsigma) + \frac{bc}{d}\right] \tag{23}$$

$$\Psi_h(\varsigma) = -\left[\left(1 + \frac{2a}{3}\varsigma\right)^{1.5} + b\left(\varsigma - \frac{c}{d}\right)\exp(-d\varsigma) + \left(\frac{bc}{d} - 1\right)\right] \tag{24}$$

where $a = 1$, $b = 0.667$, $c = 5$, $d = 0.35$.

The Monin–Obukhov stability parameter was computed as follows:

$$\varsigma = \frac{z}{L} \tag{25}$$

where $L$ is the Monin–Obukhov length (m) computed by means of the following equation (Kalma 1989):

$$L = \frac{u_*^3 pc_p(T_a + 273.16)}{kgH} = \frac{u_*^2(T_a + 273.16)}{kgT_*} \tag{26}$$

where $u_*$ is the wind friction velocity (m $s^{-1}$), $\rho$ is the air density (kg $m^{-3}$), $c_p$ is the specific heat at constant pressure (J $kg^{-1}$ $K^{-1}$), $g$ is the acceleration due to gravity (m $s^{-2}$) and $T_*$ is a scaling parameter in the boundary layer, analogous to the friction velocity (°C).

The wind friction velocity was computed by the equation given below (Kalma 1989):

$$u_* = \frac{kU}{ln\frac{z-d}{z_{0m}} - \Psi_m(\varsigma)} \tag{27}$$

and $T_*$ using the following formula (Kalma 1989):

$$T_* = \frac{k(T_a - T_s)}{ln\frac{z-d}{z_{0h}} - \Psi_h(\varsigma)} \tag{28}$$

All stability parameters, the Monin–Obukhov length, the friction velocity and the scaling parameter $T_*$ were computed by means of the iterative procedure proposed by Itier [1980, cited in Kalma (1989)]. For more details, see Kalma (1989) and Liu et al. (2007).

Bulk surface resistance was calculated according to the Penman–Monteith equation (Jackson et al. 1981; Wallace 1995); we used the following modification:

$$r_c = r_a \frac{\frac{\gamma r_a(R_n - G)}{pc_p} - (T_c - T_a)(\Delta + \gamma) - VPD}{\gamma\left[(T_c - T_a) - \frac{r_a(R_n - G)}{(pc_p)}\right]} \tag{29}$$

The mean values reported in Tables 3, 4, 5, 6 and 7 were derived from 24-hour data. Linear analysis was used to assess existing correlation between time and individual meteorological parameters and between time and energy fluxes. A confidence interval of 95 % was used, and $p$ values <0.05 were considered significant.

## Results

### Micrometeorological parameters

The monthly values of incoming solar radiation ($R_{s\downarrow}$) for year 2008 (from January to December) were 145, 146, 132 and 123 kWh $m^{-2}$ for May, June, July and August, respectively (Fig. 2).

The daily time courses of $R_{s\downarrow}$ were similar at all sites and reached a maximum of about 900 W $m^{-2}$ (Fig. 3a). The monthly average fluxes of $R_{s\downarrow}$ (W $m^{-2}$) for all the sites (Table 3) were the highest in June when mean values fluctuated from 300 W $m^{-2}$ in the wet meadow to 314 W $m^{-2}$ in the pasture. The average values of $R_{s\downarrow}$ on sunny days for time period from May to August ranged between 291 (wet meadow) and 300 W $m^{-2}$ (pasture).

The amount of reflected shortwave solar radiation ($R_{s\uparrow}$) differed markedly between the different sites (Fig. 3b). The highest reflection, up to 230 W $m^{-2}$, was measured over the concrete surface. The daily mean fluxes of $R_{s\uparrow}$ at the remaining sites were quite similar to each other and ranged from 152 (pasture) to 175 W $m^{-2}$ (wet meadow).

The monthly mean values of $R_{s\uparrow}$ (Table 3) showed the highest mean flux over the concrete surface (81.7 W $m^{-2}$). The mean fluxes of $R_{s\uparrow}$ at the remaining sites were close together (from 59.4 to 62.5 W $m^{-2}$). The diurnal mean time course of albedo, which is defined as the ratio of reflected to incoming solar radiation, (Fig. 4) showed 27 % at the site converted by concrete with a mean albedo for the sites with vegetation cover comprised between 20 and 21 %.

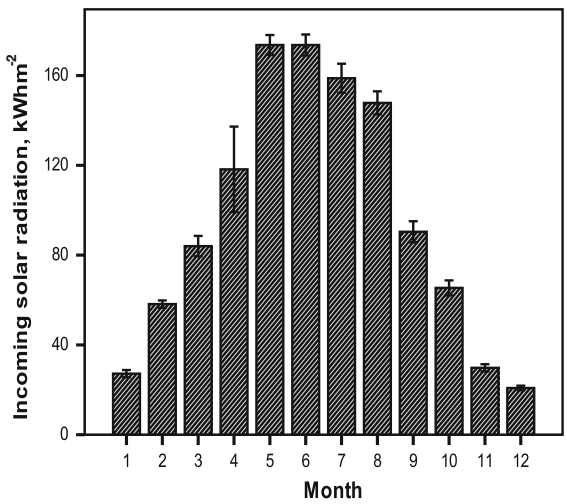


**Fig. 2** Monthly values of incoming solar radiation (kWh $m^{-2}$) data recorded for the January–December 2008 period. Mean values measured at the four sites

The high albedo values measured in the early morning and in the late afternoon were both caused by a small angle of incident solar radiation and by dividing very small numbers of both variables of the ratio: they thus do not provide much useful information (Bray et al. 1966). We neglected these values and used for calculation the values between 6:00 and 18:00 h.

The diurnal course of net radiation ($R_n$) corrected for longwave fluxes (Fig. 5a) was quite similar at the three vegetated sites, not exceeding 600 W $m^{-2}$. The maximum diurnal $R_n$ on the concrete surface was lower, with a maximum of 430 W $m^{-2}$.

The mean daily fluxes of $R_n$ for all the sites (Table 3) ranged from 153 W $m^{-2}$ (concrete surface) to 184 W $m^{-2}$ (wet meadow and pasture). The lowest $R_n$ was observed on the concrete surface, while the highest was over the vegetated sites.

The mean daily sums of $R_{s\downarrow}$, $R_{s\uparrow}$ and $R_n$ calculated from the mean fluxes at four sites on clear days are

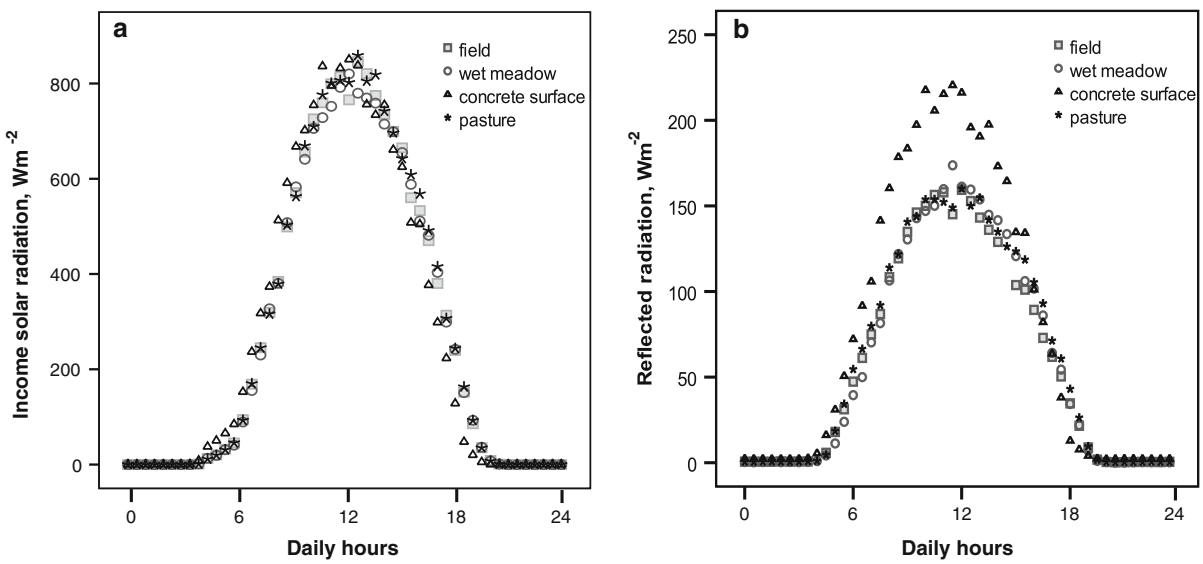


**Fig. 3** Daily mean time series of incoming solar radiation (W $m^{-2}$) (**a**) and reflected shortwave solar radiation (W $m^{-2}$) (**b**), measured on clear days during the period: 1 May– 31 August, 2008

**Table 3** Mean monthly incoming solar radiation ($Rs_{\downarrow}$, W $m^{-2}$), reflected solar radiation ($Rs_{\uparrow}$, W $m^{-2}$), net radiation ($R_n$, W $m^{-2}$), albedo (α, %) and Bowen ratio (β) during the study period

| | | $Rs_{\downarrow}$ | $Rs_{\uparrow}$ | $R_n$ | α | β |
|---|---|---|---|---|---|---|
| May | Field | 303.0 | 61.3 | 171.4 | 20.2 | 0.60 |
| | Meadow | 291.4 | 57.3 | 154.7 | 19.7 | 1.28 |
| | Pasture | 301.6 | 67.2 | 160.5 | 22.3 | 0.38 |
| | Concrete | 304.1 | 76.8 | 147.4 | 25.3 | 1.19 |
| June | Field | 304.8 | 63.1 | 173.9 | 20.4 | −0.09 |
| | Meadow | 300.3 | 68.4 | 162.1 | 22.8 | −0.05 |
| | Pasture | 313.7 | 64.7 | 190.8 | 20.6 | 0.05 |
| | Concrete | 304.4 | 84.8 | 148.6 | 27.9 | 1.21 |
| July | Field | 302.3 | 61.5 | 166.1 | 20.7 | 0.08 |
| | Meadow | 301.0 | 65.5 | 170.1 | 21.7 | −0.22 |
| | Pasture | 304.5 | 58.6 | 169.9 | 19.2 | 0.14 |
| | Concrete | 303.7 | 85.8 | 128.5 | 28.2 | 1.08 |
| August | Field | 278.4 | 51.8 | 140.0 | 18.6 | 0.89 |
| | Meadow | 269.4 | 51.6 | 155.7 | 19.2 | −0.28 |
| | Pasture | 281.0 | 59.4 | 144.9 | 21.2 | 0.41 |
| | Concrete | 278.4 | 77.5 | 111.4 | 27.8 | 1.12 |
| Overall | Field | 297.1 | 59.4 | 182.4 | 20.0 | 0.37 |
| | Meadow | 290.5 | 60.7 | 183.6 | 20.8 | 0.18 |
| | Pasture | 300.2 | 62.5 | 183.8 | 20.9 | 0.25 |
| | Concrete | 297.0 | 81.7 | 153.2 | 27.1 | 1.13 |

given in Table 4. The mean daily values of $R_{s\downarrow}$ ranged from 7.2 kWh $m^{-2}$ at the pasture to 7.0 kWh $m^{-2}$ at the wet meadow on clear days. The highest daily average of $R_{s\uparrow}$ was 1.9 kWh $m^{-2}$ at the concrete surface. The lowest average values of $R_{s\uparrow}$ were observed at the barley field (1.4 kWh $m^{-2}$). The average daily values of $R_n$ fluctuated from 4.6 kWh $m^{-2}$ (wet meadow) to 3.8 kWh $m^{-2}$ (concrete).

The daily courses of air temperature at canopy height (0.3 m) (Fig. 6a) showed that on clear days at 0.3 m, the pasture had the highest air temperature values; other sites showed similar midday temperatures, whereas the morning temperature differences between the localities were up to 8 °C. Low early morning temperatures at the wet meadow can be explained by the location of the wet meadow in a terrain depression. During the night, cold air originating from the surrounding higher ground, several metres above, flows down towards the wet meadow in the lowland surroundings. The early morning fog

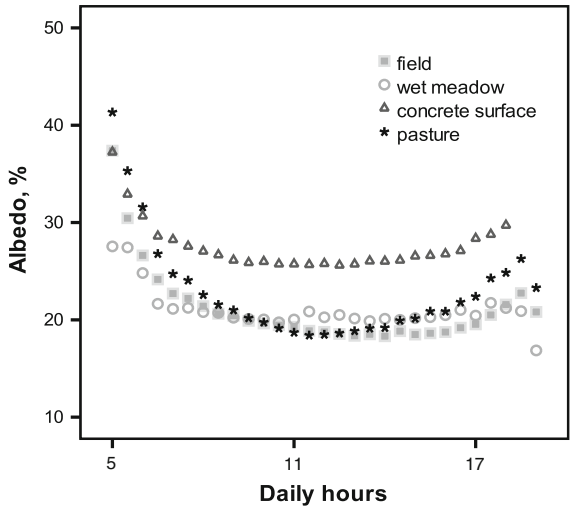


**Fig. 4** Daily series of albedo (%) measured on clear days at the four sites (the number of monitored days at each site is given in Table 2)

keeps temperature low and also provides more moisture.

On clear days, the average difference of air temperature measured at 0.3 m between the wet meadow and the concrete surface was 3.6 °C (Table 5). The average air temperatures' differences at 2-m height between the three vegetated sites was 0.6 °C (17.8 °C at the wet meadow and 18.4 °C at the pasture) (Table 5). The maximum deviation at 2-m height between the vegetated sites and the concrete surface reached 1.8 °C (17.8 °C at the wet meadow and 19.6 °C at the concrete surface). The air temperature at 0.3 m at the barley field varied from 15.1 °C (May) to 20.8 °C (August), while the canopy air temperature at the wet meadow ranged from 14.6 to 17.2 °C.

The time course of the average values of relative air humidity (RH) at 0.3 m (Fig. 6b) shows the highest values at the pasture (about 80 %) and a similar pattern at the wet meadow. The mean values of RH at 2 and 0.3 m (Table 5) showed the highest RH (80 %) at 0.3 m in the pasture and the lowest (75 %) in the field. In contrast, the pasture, the wet meadow and the field had values of mean RH close to each other at 2 m on clear days (67.7, 69.0 and 68.4 %, respectively). Differences in RH were probably caused by a different development of the vegetation cover (above ground biomass, LAI) and of the soil water content during the vegetated season.

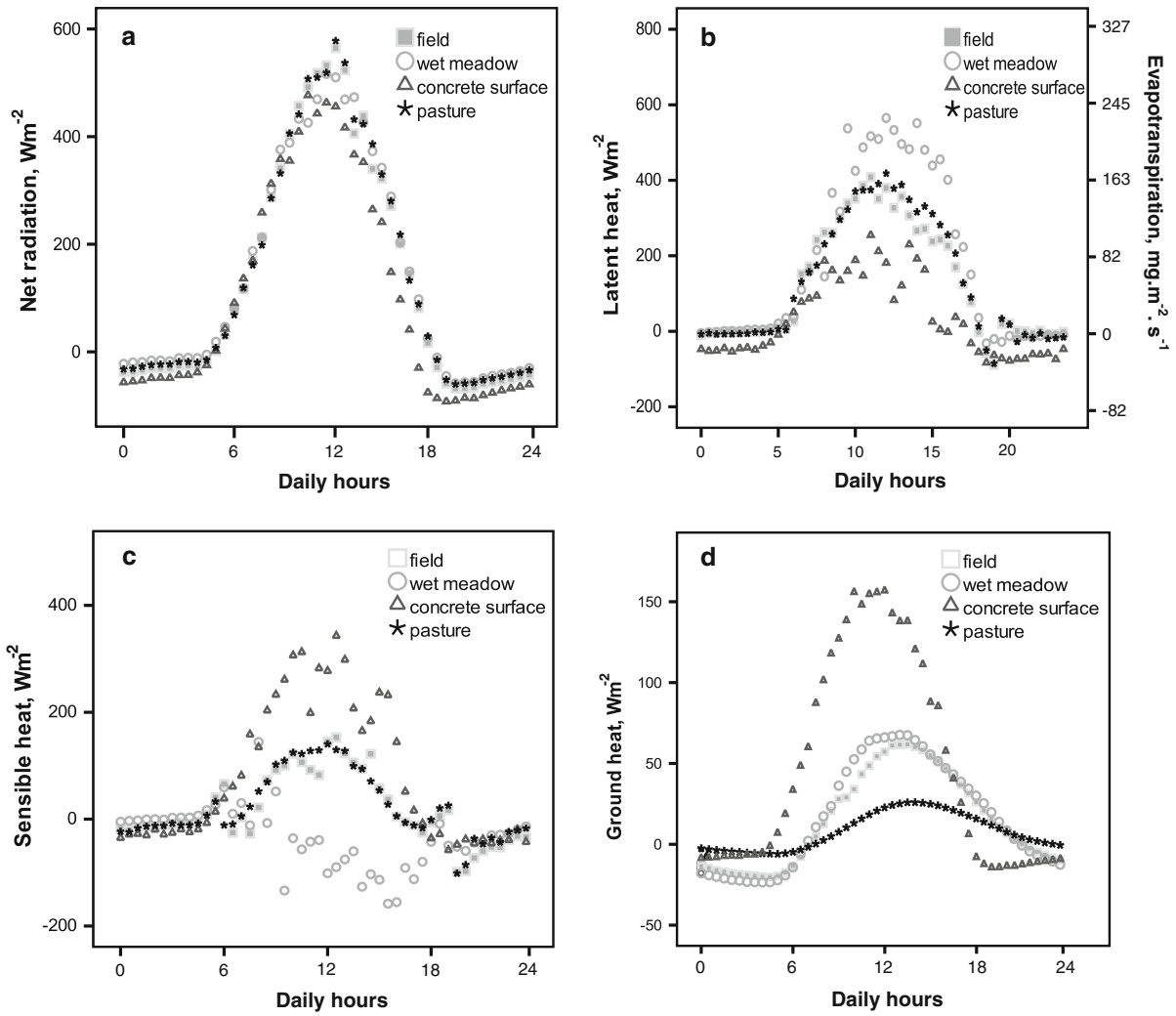


**Fig. 5** Daily mean series of total net radiation (W $m^{-2}$) (**a**), latent heat flux (W $m^{-2}$) and evapotranspiration of water (mg $m^{-2}$ $s^{-1}$) (**b**), sensible heat flux (W $m^{-2}$) (**c**), and ground heat flux (W $m^{-2}$) (**d**) on clear days from 1 May to 31 August 2008 (the number of monitored days at each site are given in Table 2)

**Table 4** Mean daily incoming solar radiation ($Rs_{\downarrow}$), reflected solar radiation ($Rs_{\uparrow}$), net radiation ($R_n$), latent heat flux (LE), sensible heat flux (H) and ground heat flux (G) (kWh $m^{-2}$)

| | Field | Wet meadow | Pasture | Concrete |
|---|---|---|---|---|
| $Rs_{\downarrow}$ | 7.02 | 7.00 | 7.20 | 7.03 |
| $Rs_{\uparrow}$ | 1.40 | 1.46 | 1.50 | 1.90 |
| $R_n$ | 4.42 | 4.59 | 4.49 | 3.78 |
| LE | 2.06 | 2.66 | 1.58 | 0.46 |
| H | 2.02 | 1.59 | 2.04 | 2.91 |
| G | 0.34 | 0.34 | 0.16 | 1.12 |

## Variation in energy fluxes

The way in which $R_n$ was processed differed amongst sites (Table 6). The energy involved in evapotranspiration ranged between 25.6 W $m^{-2}$ (concrete surface) and 164.7 W $m^{-2}$ (wet meadow). The monthly mean latent heat fluxes (LE) values were similar in the field and in the pasture (134.8 and 143.5 W $m^{-2}$, respectively). The ground heat fluxes (G), which represent the smallest component of $R_n$, ranged from 7.1 W $m^{-2}$ (pasture) to 38.5 W $m^{-2}$ (concrete surface). The evaporative fraction

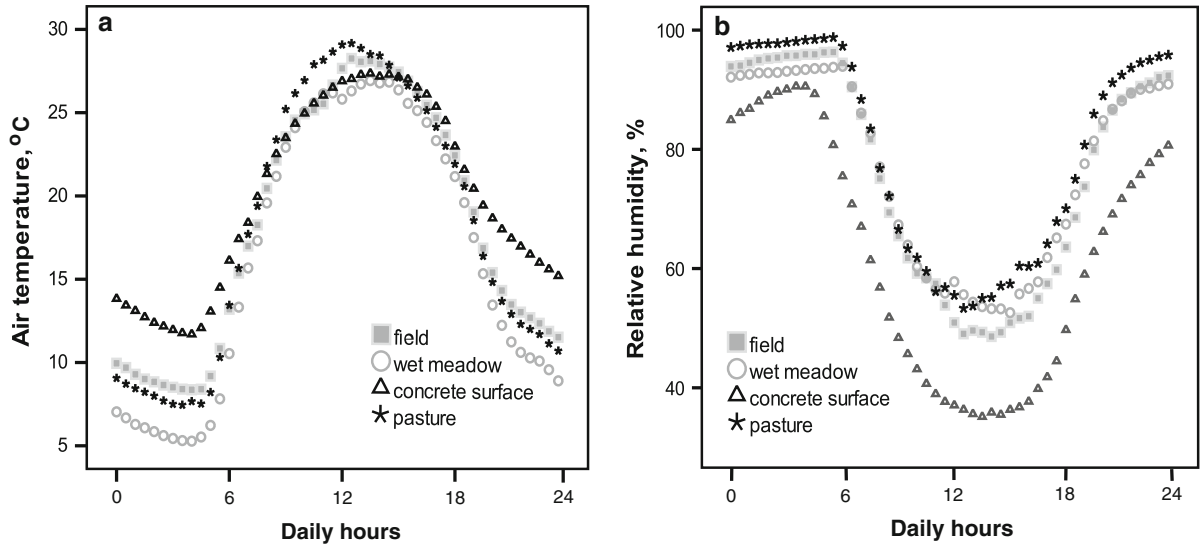


**Fig. 6** Daily mean time series of air temperature (°C) (**a**) and relative air humidity (%) (**b**), measured at canopy height (0.3 m) on clear days calculated from 1 May to 31 August 2008

**Table 5** Monthly mean air temperature (°C ± SD) and relative air humidity (% ± SD) at 2 m ($T_a$, $RH_a$) and 0.3 m ($T_s$, $RH_s$) for all sites from 1 May to 31 August 2008

| | | $T_a$ | $T_s$ | $RH_a$ | $RH_s$ |
|---|---|---|---|---|---|
| May | Field | 14.7 | 15.1 | 71.2 | 75.2 |
| | Meadow | 14.9 | 14.6 | 68.0 | 69.1 |
| | Pasture | 15.5 | 15.1 | 68.5 | 76.3 |
| | Concrete | 16.8 | 17.0 | 62.3 | 61.6 |
| June | Field | 19.5 | 18.6 | 69.3 | 80.8 |
| | Meadow | 19.4 | 18.1 | 70.1 | 81.0 |
| | Pasture | 20.2 | 19.9 | 68.1 | 84.8 |
| | Concrete | 21.1 | 21.4 | 62.6 | 61.7 |
| July | Field | 19.9 | 19.3 | 65.1 | 78.6 |
| | Meadow | 19.2 | 16.7 | 68.4 | 82.6 |
| | Pasture | 19.5 | 19.5 | 67.4 | 82.3 |
| | Concrete | 20.7 | 21.4 | 61.9 | 61.1 |
| August | Field | 20.0 | 20.8 | 64.2 | 66.9 |
| | Meadow | 19.6 | 17.2 | 70.0 | 77.4 |
| | Pasture | 19.2 | 19.1 | 69.6 | 75.2 |
| | Concrete | 20.9 | 21.6 | 63.5 | 61.8 |
| Overall | Field | 18.2 | 18.2 | 67.7 | 75.3 |
| | Meadow | 17.8 | 16.4 | 69.0 | 76.5 |
| | Pasture | 18.4 | 18.1 | 68.4 | 79.4 |
| | Concrete | 19.6 | 20.0 | 62.6 | 61.6 |

(EF) [i.e. the ratios of evapotranspiration to available energy at the ground surface (Rn − G)] ranged from 0.22 (concrete) to 1.04 (wet meadow).

The hourly energy fluxes measured on clear days at canopy height level in the four sites (Fig. 5) reached value of several 100 W $m^{-2}$. At all sites, LE flux peaked in the afternoon, while the minimum was observed during the night. Mean daytime LE reached a maximum of about 630 W $m^{-2}$ (wet meadow). Mean diurnal LE reached similar values (ca. 400 W $m^{-2}$) at the pasture and at the field, while at the concrete surface it did not reach 230 W $m^{-2}$. At the wet meadow, most of $R_n$ was converted into LE; conversely, at the concrete surface, sensible heat (H) was the dominant flux measured (up to 370 W $m^{-2}$). At all vegetated sites, H was relatively low (less than 220 W $m^{-2}$), whereas LE fluxes reached a maximum comprised between 400 and 600 W $m^{-2}$, which corresponds to ET rates of up to 0.15 g $m^{-2}$ $s^{-1}$. The highest diurnal G was up to 150 W $m^{-2}$ at the concrete surface, 40 W $m^{-2}$ at the wet meadow, 40 W $m^{-2}$ at the field and 18 W $m^{-2}$ at the pasture.

The mean daily sums of LE, H and G calculated from the mean fluxes measured at the four sites on clear days are reported in Table 4. The mean daily LE values ranged from 2.7 kWh $m^{-2}$ at the wet meadow to 0.5 kWh $m^{-2}$ at the concrete surface on clear days. The highest daily average H was 2.9 kWh $m^{-2}$ at the concrete surface, while the lowest average H was observed at the wet meadow (1.6 kWh $m^{-2}$). The daily average G values ranged from 0.2 kWh $m^{-2}$ (pasture) to 1.1 kWh $m^{-2}$ (concrete).

**Table 6** Monthly mean values of energy balance component, evaporative fraction (EF) and evapotranspiration (ET) during the measurement period

| | | Fluxes (W $m^{-2}$) | | | | EF | ET (mm) |
|---|---|---|---|---|---|---|---|
| | | LE | H | $R_n$ | G | | |
| May | Field | 138.9 | 82.7 | 241.7 | 20.1 | 0.63 | 4.9 |
| | Meadow | 94.4 | 120.8 | 234.1 | 18.9 | 0.44 | 3.3 |
| | Pasture | 164.8 | 62.5 | 234.3 | 7.0 | 0.73 | 5.8 |
| | Concrete | 44.5 | 114.6 | 227.3 | 68.2 | 0.28 | 1.6 |
| June | Field | 186.1 | −16.1 | 181.7 | 11.7 | 1.09 | 6.6 |
| | Meadow | 165.6 | −8.2 | 174.5 | 17.1 | 1.05 | 5.8 |
| | Pasture | 168.3 | 9.2 | 185.9 | 8.4 | 0.95 | 5.9 |
| | Concrete | 33.4 | 69.4 | 146.5 | 43.7 | 0.32 | 1.2 |
| July | Field | 146.5 | 11.8 | 166.1 | 7.8 | 0.93 | 5.2 |
| | Meadow | 202.3 | −44.5 | 170.1 | 12.3 | 1.28 | 7.1 |
| | Pasture | 142.8 | 20.7 | 169.9 | 6.4 | 0.87 | 5.0 |
| | Concrete | 32.7 | 56.8 | 128.1 | 38.6 | 0.37 | 1.2 |
| August | Field | 67.5 | 59.9 | 140 | 12.6 | 0.53 | 2.4 |
| | Meadow | 196.3 | −54.4 | 155.7 | 13.8 | 1.38 | 6.9 |
| | Pasture | 98.1 | 40.3 | 144.9 | 6.5 | 0.71 | 3.5 |
| | Concrete | −18.8 | 96.8 | 111.4 | 33.4 | −0.24 | −0.7 |
| Overall | Field | 134.8 | 34.6 | 182.4 | 13.1 | 0.80 | 4.8 |
| | Meadow | 164.7 | 3.4 | 183.6 | 15.5 | 1.04 | 5.8 |
| | Pasture | 143.5 | 33.2 | 183.8 | 7.1 | 0.82 | 5.1 |
| | Concrete | 25.6 | 89.0 | 153.1 | 38.5 | 0.22 | 0.9 |

The dissipation of $R_n$ was calculated for each site (Fig. 7). The wetland had the highest $LE/R_n$ (0.90), while midrange values of $LE/R_n$ were recorded at the pasture and at the field (0.79 and 0.75, respectively), while the artificial concrete surface had the lowest $LE/R_n$ (0.26). At all sites, $G/R_n$ ranged from 0.06 to 0.10.

The mean aerodynamic resistance ($r_a$), bulk surface resistance ($r_c$), vapour pressure deficit (VPD), available energy (Rn − G) and decoupling coefficient (Ω), assessed during three separate periods (Table 7), were in the ranges of 122–257, 73–229, and 96–315 s $m^{-1}$ for the field, the wet meadow and the pasture, respectively, between 10:00 and 16:00. The relationship amongst surface resistance, available energy, vapour pressure deficit and air temperature at the three vegetated sites (Fig. 8) showed that $r_c$ increased linearly with the increasing VPD ($R_2 = 0.60$, $df = 1$, 289, $p < 0.001$ (field); $R_2 = 0.46$, $df = 1$, 301, $p < 0.001$ (wet meadow); $R_2 = 0.55$, $df = 1$, 291, $p < 0.001$ (pasture) (Fig. 8a). The surface resistance also increased linearly with the increasing air temperature ($R_2 = 0.32$, $df = 1$, 289, $p < 0.001$ (field); $R_2 = 0.44$, $df = 1$, 301, $p < 0.001$ (wet meadow); $R_2 = 0.41$, $df = 1$, 291, $p < 0.001$ (pasture) (Fig. 8b). Surface resistance rose in parallel to an increase in available energy (Fig. 8c); however, the slope of the regression line was low.

Mean $r_a$ values had a small variation and were in the ranges of 30–61, 35–48, and 41–80 s $m^{-1}$ at the field, the wet meadow and the pasture, respectively. The mean values of wind speed did not exceed 3.5 m $s^{-1}$. The decoupling coefficient varied little between different periods (Table 7). Mean values were between 0.60 and 0.83, 0.65 and 1.23, 0.80 and 0.89 for field, wet meadow and pasture, respectively. The highest mean values of Ω were observed in July at the field and at the pasture. At the wet meadow, in August, Ω exceeded 1.

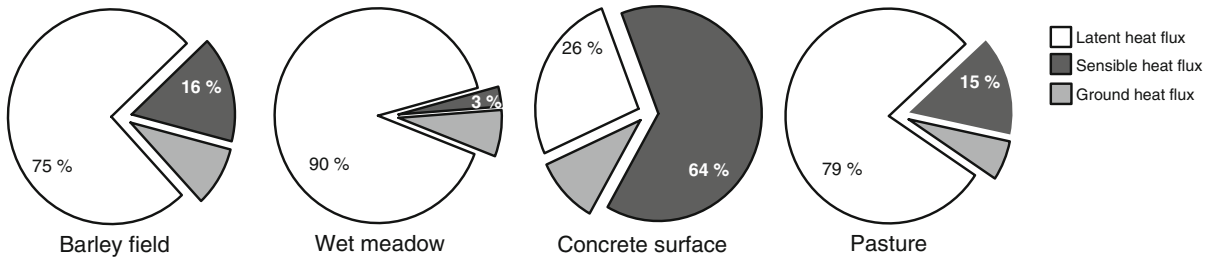


**Fig. 7** Dissipation of net radiation (%) amongst latent heat, sensible heat and ground heat fluxes on clear days from 1 May to 31 August 2008

**Table 7** Diurnal average values of wind velocity ($u_z$), surface ($r_c$, s $m^{-1}$) and aerodynamic resistance ($r_a$, s $m^{-1}$), vapour pressure deficit (VPD, kPa), available energy ($R_n - G$, W $m^{-2}$) and decoupling coefficient (Ω) for three periods between 10:00–16:00

| | | $u_z$ | $r_a$ | $r_c$ | VPD | $R_n - G$ | Ω |
|---|---|---|---|---|---|---|---|
| 23.05–25.05 | Field | 1.2 ± 0.5 | 30.3 ± 69.3 | 121.8 ± 93.2 | 1.0 ± 0.4 | 301.9 ± 198.1 | 0.79 |
| | Meadow | 1.1 ± 0.4 | 47.9 ± 64.5 | 122.2 ± 157.3 | 1.1 ± 0.4 | 302.1 ± 180.3 | 0.65 |
| | Pasture | 0.9 ± 0.5 | 80.3 ± 113.9 | 53.1 ± 115.4 | 1.1 ± 0.3 | 358.1 ± 193.3 | 0.84 |
| 01.07–03.07 | Field | 1.9 ± 0.7 | 31.9 ± 21.0 | 257.6 ± 133.5 | 2.4 ± 0.6 | 540.6 ± 240.0 | 0.83 |
| | Meadow | 1.2 ± 0.5 | 45.8 ± 67.8 | 229.4 ± 178.3 | 2.3 ± 0.6 | 509.3 ± 184.2 | 0.88 |
| | Pasture | 1.8 ± 0.7 | 40.7 ± 31.2 | 315.3 ± 180.7 | 2.3 ± 0.5 | 589.9 ± 198.9 | 0.89 |
| 06.08–08.08 | Field | 3.3 ± 1.4 | 61.1 ± 30.5 | 179.8 ± 54.4 | 1.8 ± 0.8 | 428.6 ± 176.0 | 0.60 |
| | Meadow | 1.5 ± 0.8 | 34.7 ± 46.1 | 73.0 ± 58.1 | 1.8 ± 0.7 | 437.1 ± 175.2 | 1.23 |
| | Pasture | 3.3 ± 1.4 | 49.8 ± 106.7 | 95.6 ± 80.4 | 1.8 ± 0.5 | 505.6 ± 181.6 | 0.80 |

## Discussion

### Monitored data and evaluated energy fluxes

Evapotranspiration occupies a central role in the processing of water and energy fluxes within ecosystems. The most powerful fluxes of energy dissipation on clear days are linked to sensible heat and/or to latent heat of evapotranspiration. Our results clearly show how, depending on the availability of water and vegetation, different land cover types convert solar energy in different ways. During dry spells, at the wet meadow, more than 100 % of net radiation is dissipated through evapotranspiration. These values indicate that at the wet meadow, up to 70 % more energy was converted into latent heat of evapotranspiration than at the concrete surface site, and up to 30 % more than at the pasture or at the barley field. Many physical and biological factors, such as leaf area index, available energy, soil moisture ability, plant physiology, production characteristics and vapour pressure deficit, bear an influence on energy dissipation (Liu et al. 2009). A high dissipation of latent heat flux (LE/$R_n$) at the wet meadow site can be explained because of high moisture availability and to low surface resistance to evaporation. The midrange values recorded at the field and at the pasture sites are due to the nature of their vegetation cover and to the higher surface resistance which counterbalanced the high amount of available moisture. Small dissipation of LE/$R_n$ values at the concrete surface site are caused by the absence of vegetation and the small water holding capacity. On the whole, at all vegetated sites, LE/$R_n$ exceeded 0.70. These data demonstrated that evapotranspiration is a major component of the energy balance under dry hot days in our region. Similar results were found at the tropical prairie wetland in north-central Florida, USA, where approximately 64 % of net radiation was dissipated through evapotranspiration, and 32 % was converted into sensible heat (Jakobs et al. 2002).

Evapotranspiration rates which we measured at the wet meadow ranged from 3.3 to 7.1 mm $d^{-1}$. In similar geographical zone, Burba et al. (1999)

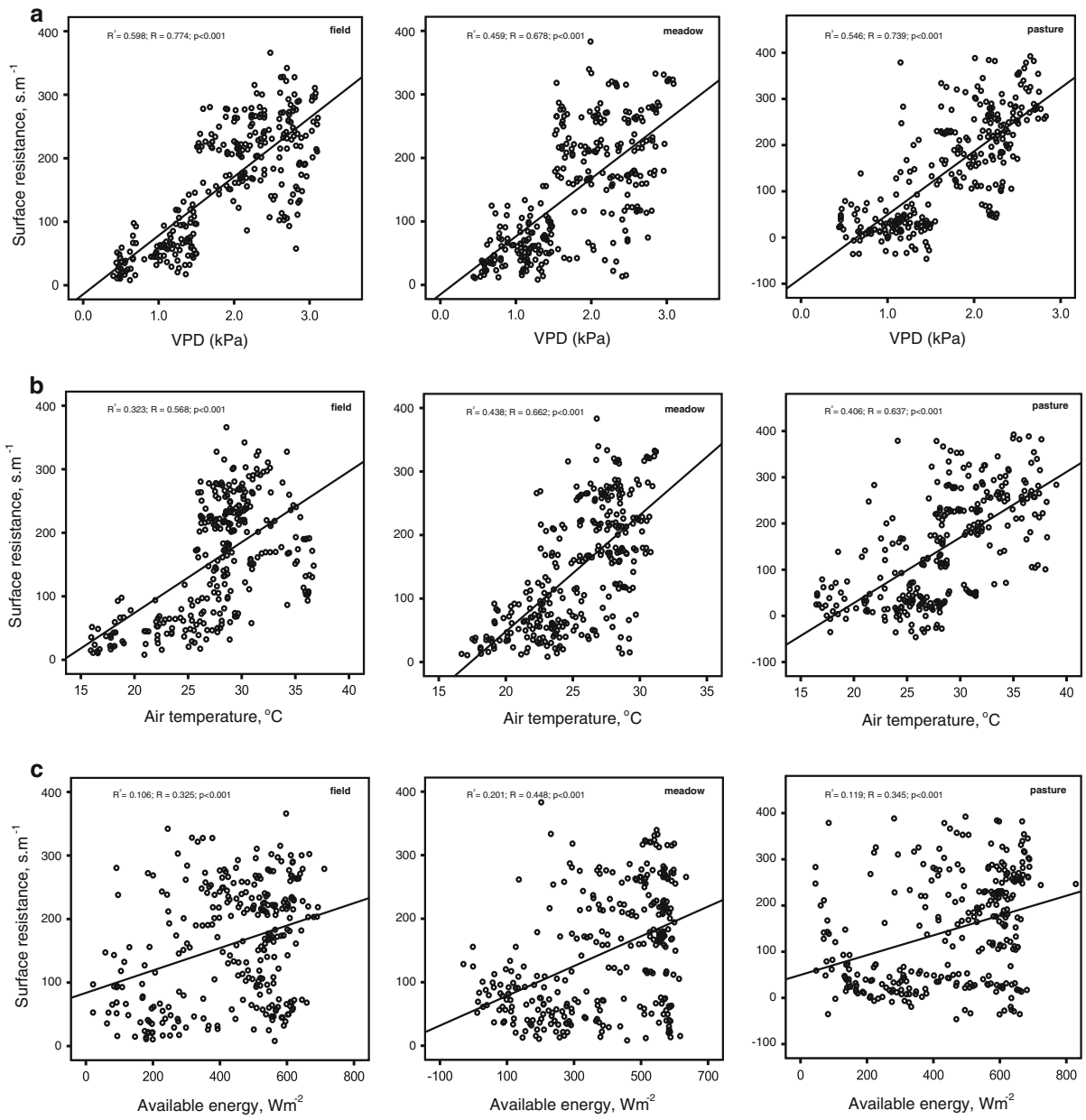


**Fig. 8** Relationship between surface resistance (s $m^{-1}$) and water VPD (kPa) (**a**), air temperature (°C) (**b**), and available energy (W $m^{-2}$) (**c**) for the three vegetated sites

measured 3.5–6.5 mm $d^{-1}$ at a prairie wetland site in Nebraska, USA. Peacock and Hess (2004) measured 0.5–5.5 mm $d^{-1}$ in Kent, UK, while Zhou and Zhou (2009) observed between 0.1 and 5.8 mm $d^{-1}$ in reed beds during the growing season in the Liaohe Delta, Northeast China. By comparison, evapotranspiration rates over the Amazonian forest varied between 2 and 6 mm $d^{-1}$ and between 0.4 and 5 mm $d^{-1}$ during the wet and the dry seasons, respectively (Sanches et al. 2011).

Blad and Rosenberg (1976); Brakke et al. (1978); Monteith (1981); Oke (1987); Guo and Schuepp (1994); Lee et al. (2004); Ryszkowski and Kedziora (2007) showed that local heat advection contributed to increased evaporation and/or evapotranspiration. Advection takes place when sensible heat flux is

negative at or near the ground level (McNaughton and Jarvis 1983). Horizontal advection transfers heat from higher to lower temperatures because of the canopy–air temperature differences (Li and Yu 2007). Our results showed such a temperature gradient between the agricultural landscapes and the wet meadow. The negative sensible heat values observed at the wet meadow site indicate the presence of temperature inversion caused by the advection of warm air from surrounding areas which tends to occur during clear days. Guo and Shuepp (1994) stressed that the evapotranspiration at wetland sites can be enhanced by local heat advection from neighbouring areas by more than 20 %. Brakke and Verma (1978) found that sensible heat advection provided about 50 % of the total energy dissipated through evapotranspiration. The process of dry air advection from a field to a hedgerow was described by Ryszkowski and Kedziora (2007). At the cultivated field, more net radiation was converted into sensible heat than at the forest. A temperature gradient was measured between the field and the hedgerows proving that heat advection occurred. Our results correspond well to the results obtained at a temperate wetland under hot summer conditions measured by Rejšková et al. (2010). In their study, the evaporative fraction reached values higher than 1.0 in the afternoon hours of a hot day because of advection.

The surface reflectance (albedo) depends on the vegetation cover, namely, on its biomass and on its water content. Lafleur et al. (1987) reported an average albedo of 11–20 % for sedge-dominated wetlands, while Burba et al. (1999) reported an albedo of 12–16 % for common reed. In our study, the albedo for the vegetated sites is in agreement with the results by Brunsell et al. (2011), where the variation of the albedo ranged from 18 to 25 % as a function of vegetation cover.

Low albedo was associated with high values of $LE/R_n$ (wet meadow), while high albedo was associated with low $LE/R_n$. The values of EF varied from site to site; at the wet meadow, EF was the highest with 1.04, a value which is well above the EF (0.84) reported at the wet meadow studied by Ryszkowski and Kedziora (1987). At the concrete surface, EF was 0.30, which was comparable to the urban surface (0.29) reported by Coutts et al. (2007). At the pasture, EF was slightly higher (0.82) in comparison to the EF values of observed at the pasture (0.55) by Wang et al. (2006). This difference could be explained by a higher groundwater level at our pasture site.

Crop resistance ($r_c$) is related to the available energy for evapotranspiration ($Rn - G$), temperature gradient, the vapour pressure deficit (VPD) and aerodynamic resistance of the surface (Jackson et al. 1981; Wallace 1995). The decrease of $r_c$ is related to an increase in irradiance, and it rises with increasing VPD (McNaughton and Jarvis 1983). Our results indicate that $r_c$ is more sensitive to VPD and to temperature than to the amount of available energy. Doorenbos and Pruitt (1977) reported a standard $r_c$ value for grass of 70 s $m^{-1}$. The $r_c$ above the wet grassland fluctuated between 50 and 100 s $m^{-1}$ (Acreman et al. 2003; Jakobs et al. 2002). Wessel and Rouse (1994) reported that $r_c$ can vary between as much as 29 and 251 s $m^{-1}$.

## Effect of ET on local climate and water cycle

Our results document a striking difference in the seasonal energy balance measured at the four sites with only a few kilometres between each other. Under hot weather conditions, the wet meadow showed a high capacity of energy conversion into latent heat of water vaporisation. Wetlands can compensate for temperature rises because of warm dry air by increasing their evapotranspiration rate, which can be even higher than the value of net radiation at the wetland site. Different ET rates result in differences in land covers surface temperature at vegetation (canopy) height. In other words, the temperature measured at the height of the dominant vegetation in various vegetated sites can serve as an indicator of the rate of evapotranspiration. A detailed study of daily dynamics of radiation surface temperature of seven types of land cover in a cultural temperate landscape showed a difference of up to 20 °C between different types of vegetation supplied with water and drained areas (Hesslerová et al. 2013).

The excess of heat and the lack of water over arable fields dramatically reduce crop yields, while wetlands play a very important role in moderating the water cycle and retaining water within the catchment. The structure of agricultural landscapes bears important linkages with the local climate. Restoring wetlands next to agricultural plots could be an effective measure for managing the heat balance of the landscape. The average maximum ET during clear days is a

demonstration of the role of vegetation in dampening temperature differences caused by surplus solar radiation and in shaping microclimate and mesoclimate conditions. Within wet meadows, ET reaches ca. 600 W $m^{-2}$, which when projected over 1 $km^{-2}$, corresponds to 600 MW—the efficiency of a midsized electricity generating power station. ET equalises temperature differences within the landscape both in space and in time. Transpiration is driven by conversion of solar energy into latent heat of water vaporisation. Energy used for water vaporisation does not increase ambient temperature; the energy is hidden (latent) in kinetic movement of molecules of water vapour. When temperature drops below the dew point, water vapour condensates, and latent heat is released. Transpiration is a cooling process (endothermic), whereas condensation of water vapour is on the opposite a warming process (exothermic). The water cycle (water vaporisation–water vapour condensation) is a process equalising temperature differences (lowering heat potentials); plants can be considered as processors controlling the equalisation of temperature differences. There are up to several 100 stomata for every $mm^2$ of leaf surface; each stoma functions like a valve controlling the uptake of carbon dioxide and the release of water vapour.

The cooling process of transpiration is often considered a side effect rather than a mechanism to control leaf temperature (Lambers et al. 1998). Transpiration is also perceived as a rather negative process. Plant physiologists and hydrologists may use negative terms such as 'transpiration loss' and 'evapotranspiration losses'.

A similarly great controversy exists at present in the discussions about the functioning of forests' and their role in the hydrological cycle. Transpiration is sometimes even considered an unavoidable evil, in the sense that water is sacrificed for the sake of enabling intake of $CO_2$ for photosynthesis to occur. When comparing relatively small catchments, less rainfall is converted into runoff from afforested catchments than from grass covered or partly drained catchments (Andreassian 2004). On the other hand, large scale deforestation has often been linked to less precipitation and to regional shortages of water (Ponting 1993, Diamond 2005).

Makarieva and Gorshkov (2007) point out that, in forest-covered regions, annual precipitation does not decline with the increasing distance from the ocean, and may even rise as one proceeds several 1000 km inland. By contrast, where forests are lacking, precipitation decreases exponentially over just a few 100 km. They coined the term 'biotic pump' of atmospheric moisture to designate the biotically induced atmospheric circulation sustaining the hydrological cycle on land (Makarieva and Gorshkov 2007). Their initial theory has more recently been supported by new evidence (Makarieva et al. 2013). In this last publication, they point to the inversion of temperature that occurs in a structured forest canopy in comparison with simple crop plants: there is higher temperature in tree crowns than in the herb and shrub layers. As heavier, colder air remains at ground level, water vapour may condense over herbs and shrubs even during a sunny day. When the temperature goes down at night, the air becomes more saturated and condensation occurs above the tree canopy. Condensation of water vapour results in a decrease of air pressure, such that air from surrounding areas is sucked in. According to Makarieva and Gorshkov (2007), vegetate dares as characterised by intense evapotranspiration constitute 'acceptor regions' of low atmospheric pressure on land which attract water vapour. On the other hand, dry, overheated areas function as 'donor regions'; they lose water transported in turbulent fluxes of hot air (sensible heat). Such overheated areas are prone to the rapid decomposition of organic material, loss of nutrients and erosion (Ripl 2003; Hesslerová et al. 2013).

In an agricultural landscape, wetlands provide a climate regulation service, which is linked to closed water cycles, nutrient retention, biomass and oxygen production (Seják et al. 2012). Climate regulation is a critical regulatory ecosystem service provided by wetlands, which dampens temperature differences within the landscape. This ecosystem service can be expressed in monetary terms by relating it to the cost of the electricity that would be consumed for providing this air-conditioning effect artificially. Each $m^2$ from 500 l water evaporate annually would require an investment of 70 USD (i.e. 0.7 kWh cooling + 0.7 kWh warming × 0.1 USD × 500 l).

The Unites States have lost over half of their wetlands since Independence was declared (Dahl 2011). The wetland surface area deceased from 200 million ha in 1780 to 100 ha in 2,000—a loss of 247 million acres. Seven states—Indiana, Illinois, Iowa, Missouri, Ohio and California—have lost over 90 % (http://www.wetland.org/101/WET101C.pdf).

Johnston (2013) found wetland losses continued at a rate of 15,000 acres a year between 2001 and 2011 because of row crop expansion. In the Czech Republic, about 1 million ha of wetlands and wet meadows were drained between the 1950s and the end of the 1980s under the Socialist Regime. The decrease of ET of 100 W $m^2$ corresponds to release of 100 MW of sensible heat from 1 $km^2$. The drainage of a million ha (10,000 $km^2$) results in the release of 1 million MW of sensible heat on sunny days, which increases temperature and accelerates the transport of water vapour into the higher layers of the atmosphere. The restoration of wetlands in the agricultural landscape is therefore necessary not only for the retention of nutrients (N, P) and for carbon sequestration, but is also essential for the dampening of heat extremes and for equalising temperature differences.

**Acknowledgments** The study was supported by the National Research Program MSMT Czech Republic (NPV 2B06023) and by the South Bohemia University Grant GAJU 152/2010/Z. The authors express their gratitude to colleagues from ENKI, o.p.s. and to the staff of the company Fiedler & Mágr who maintain and manage the network of meteorological stations including the database. The authors would like to thank anonymous reviewers and editors for their helpful and constructive comments that greatly contributed to improve the final version of the article.

## References

Acreman MC, Harding RJ, Lloyd CR, McNeil DD (2003) Evaporation characteristics of wetlands: experience from a wet grassland and a reedbed using eddy correlation measurements. Hydrol Earth Syst Sci 7(1):11–21

Allen RL, Pereira DR, Smith M (1998) Crop evapotranspiration: guidelines for computing crop water requirements. Food and Agriculture Organization of the United Nations (FAO) Irrigation and Drainage Paper No. 56. Rome, FAO

Andreassian V (2004) Water and forests: from historical controversy to scientific debate. J Hydrol 291:1–27

Asrar G, Kanemasu ET (1983) Estimating thermal diffusivity near the soil surface using Laplace transform: uniform initial conditions. Soil Sci Soc Am J 47:397–401

Beljaars CCM, Holstag AAM (1991) Flux parameterization over land surfaces for atmospheric models. J Appl Meteorol 30:327–341

Blad BL, Rosenberg NJ (1976) Evaluation of resistance and mass transport evapotranspiration models requiring canopy temperature data. Agron J 68:764–769

Blanken PD, Black TA, Yang PC, Neumann HH, Nesic Z, Staebler R, den Hartog G, Novak MD, Lee X (1997) The energy balance and canopy conductance of a boreal aspen forest: partitioning overstory and understory components. J Geophys Res 102:28915–28927. doi:10.1029/97JD00193

Blanken PD, Williams MW, Burns SP, Monson RK, Knowles J, Chowanski K, Ackerman T (2009) A comparison of water and carbon dioxide exchange at a windy alpine tundra and subalpine forest site near Niwot Ridge, Colorado. Biogeochemistry 95:61–76. doi:10.1007/s10533-009-9325-9

Bowen IS (1926) The ratio of heat losses by conduction and evaporation from any surface. Phys Rev 27:779–789

Brakke TW, Verma SB, Rosenberg NJ (1978) Local and regional components of sensible heat advection. J Appl Meteorol 17:955–963. doi:10.1175/1520-0450-017

Bray J, Sanger J, Archer A (1966) The visible albedo of surfaces in central Minnesota. Ecology 47(4):524–531

Brom J, Pokorný J (2009) Temperature and humidity characteristics of two willow stands, a peaty meadow and a drained pasture and their impact on landscape functioning. Boreal Environ Res 14:389–403

Brunsell NA, Schymanski SJ, Kleidon A (2011) Quantifying the thermodynamic entropy budget of the land surface: is this useful? Earth Syst Dyn 2:87–103. doi:10.5194/esd-2-87-2011

Brutsaert W (1982) Evaporation into the atmosphere: theory, history, and application. D. Reidel Publishing Co., Dordrecht

Buck Research Manual (1996) Updated equation from Buck AL. 1981. New equations for computing vapor pressure and enhancement factor. J Appl Meteorol 20:1527–1532. doi:10.1175/1520-0450(1981)-020

Burba GG, Verma SB (2005) Seasonal and interannual variability in evapotranspiration of native tallgrass prairie and cultivated wheat ecosystems. Agr Forest Meteorol 135:190–201. doi:10.1016/j.agrformet.2005.11.017

Burba GG, Verma SB, Kim J (1999) Surface energy fluxes of *Phragmites australis* in a prairie wetland. Agr Forest Meteorol 94:31–51

Capra F (1996) The web of life: a new synthesis of mind and matter. Harper, New York

Coutts AM, Beringer J, Tapper NJ (2007) Impact of increasing urban density on local climate: spatial and temporal variations in the surface energy balance in Melbourne, Australia. J Appl Meteorol Clim 46:477–493. doi:10.1175/JAM2462.1

Craft CB (1996) Dynamics of nitrogen and phosphorus retention during wetland ecosystem succession. Wetl Ecol Manag 4(3):177–187

Dahl TE (2011) Status and trends of wetlands in the conterminous United States 2004 to 2009. U.S. Department of the Interior, U.S. Fish and Wildlife Service, Washington, DC

De Vries DA (1963) Thermal properties of soil. In: van Wijk WR (ed) Phys Plant Environ. North-Holland, Amsterdam

De Vries DA, Philip JR (1986) Soil heat flux, thermal conductivity and the null-alignment method. Soil Sci Soc Am J 50:12–18

Diamond J (2005) Collapse: how societies choose to fail or survive. Allan Lane, London

Doorenbos J, Pruitt WO (1977) Crop water requirements. Irrigation and drainage paper No. 24, revised. FAO, Rome

Eiseltová M, Pokorný J, Hesslerová P, Ripl W (2012) Evapotranspiration—a driving force in landscape sustainability. In: Irmak A (ed) Evapotranspiration—Remote sensing and modeling, InTech, Croatia, p 305–328. doi: 10.5772/725

Eulenstein F, Leśny J, Chojnicki BH, Kedziora A, Olejnik J (2005) Analysis of the interrelation between the heat

balance structure, type of plant cover and weather conditions. Int Agrophys 19:125–130
Fisher J, Acreman MC (2004) Wetland nutrient removal: a review of the evidence. Hydrol Earth Syst Sci 8:673–685
Foken T (2008) Micrometeorology. Springer, Berlin
Gates DM (1980) Biophysical ecology. Springer, New York
Geiger R, Aron RH, Todhunter P (2003) The climate near the ground. Harvard University Press, Cambridge
Gentine P, Entekhabi D, Chehbouni A, Boulet G, Duchemin B (2007) Analysis of evaporative fraction diurnal behaviour. Agr Forest Meteorol 143:13–29
Gregory SV, Swanson FJ, McKee WA, Cummins KW (1991) An ecosystem perspective of riparian zones. Bioscience 41:540–551. doi:10.2307/1311607
Gu S, Tang YH, Cui XY, Kato T, Du MY, Li YN, Zhao XQ (2005) Energy exchange between the atmosphere and a meadow ecosystem on the Qinghai–Tibetan Plateau. Agr Forest Meteorol 129:175–185. doi:10.1016/j.agrformet.2004.12.002
Guo Y, Schuepp PH (1994) An analysis of the effect of local heat advection on evaporation over wet and dry surface strips. J Clim 7:641–652. doi:10.1175/1520-0442-007
Hesslerová P, Pokorný J, Brom J, Rejšková-Procházková A (2013) Daily dynamics of radiation surface temperature of different land cover types in a temperature cultural landscape: consequences for the local climate. Ecol Eng 54:145–154
Huryna H, Pokorný J (2010) Comparison of reflected solar radiation, air temperature and relative air humidity in different ecosystems: from fishponds and wet meadows to concrete surface. In: Vymazal J (ed) Water and nutrient management in natural and constructed wetlands. Springer Netherlands, Dordrecht, pp 308–326
Hussain SA, Badola R (2008) Valuing mangrove ecosystem services: linking nutrient retention function of mangrove forests to enhanced agroecosystem production. Wetl Ecol Manag 16(6):441–450
IPCC (2007) Climate changes—synthesis report. In: Pachauri RK, Reisinger A (eds), http://www.ipcc.ch. Accessed 16 February 2010
Jackson RD, Idso SB, Reginato RJ (1981) Canopy temperature as a crop water stress indicator. Water Resour Res 17:1133–1138
Jakobs JM, Mergelsberg SL, Lopera AF, Myers DA (2002) Evapotranspiration from a wet prairie wetland under drought conditions: paynes prairie preserve, Florida, USA. Wetlands 22(2):374–385
Jarvis PG, McNaughton KG (1985) Stomatal control of transpiration: scaling up from leaf to region. Adv Ecol Res 15:1–4
Johnston CA (2013) By the (disappearing?) shores of silver lake. Natl Wetl Newsl 35(1):6
Jones HG (1992) Plants and microclimate, 2nd edn. Cambridge University Press, Cambridge
Kalma JG (1989) A comparison of expressions for the aerodynamic resistance to sensible heat transfer. CSIRO Div water resourc technical memo 89(6):11
Kao J, Titus J, Zhu W (2003) Differential nitrogen and phosphorus retention by five wetland plant species. Wetlands 23–24:979–987. doi:10.1672/0277-5212(2003)-023
Kedziora A (2004) How to manage water cycles in watershed. In: Integrated watershed management – ecohydrology & phytotechology—Manual. UNESCO, Italy
Kimball BA, Jackson RD, Reginato RJ, Nakayama FS, Idso SB (1976a) Comparison of field-measured and calculated soil–heat fluxes. Soil Sci Soc Am J 40:18–25
Kimball BA, Jackson RD, Nakayama FS, Idso SB, Reginato RJ (1976b) Soil-heat flux determination: temperature gradient method with computed thermal conductivities. Soil Sci Soc Am J 40:25–28
Kopp G, Lawrence G, Rottman G (2005) The total irradiance monitor (TIM): science results. Sol Phys 230:129–139. doi:10.1007/s11207-005-7433-9
Kravčík M, Pokorný J, Kohutiar J, Kovac M, Toth E (2008) Water for the recovery of the climate. A new paradigm. Municipali and TORY Consulting, Kosice
Kurc SA, Small EE (2004) Dynamics of evapotranspiration in semiarid grassland and shrubland ecosystems during the summer monsoon season, central New Mexico. Water Resour Res 40:W09305. doi:10.1029/2004WR003068
Květ J, Lukavská J, Tetter M (2002) Biomass and net primary production in graminoid vegetation. In: Freshwater wetlands and their sustainable future: a case study of Trebon Basin Biosphere Reserve, Czech Republic, Man and the Biosphere Series. UNESCO, Paris
Lafleur P, Rouse WR, Hardill SG (1987) Components of the surface radiation balance of subarctic wetland terrain units during the snow-free season. Arctic Alpine Res 19:53–63
Lambers H, Chapin FS III, Pons TL (1998) Plant physiological ecology. Springer, Berlin
Lee XH, Yu Q, Sun XM, Liu JD, Min QW, Liu YF, Zhang XZ (2004) Micrometeorological fluxes under the influence of regional and local advection: a revisit. Agr Forest Meteorol 122:111–124. doi:10.1016/j.agrformet.2003.02.001
Lhomme JP, Elguero E (1999) Examination of evaporative fraction diurnal behaviour using a soil-vegetation model coupled with a mixed-layer model. Hydrol Earth Syst Sci 3(2):259–270
Li LH, Yu Q (2007) Quantifying the effects of advection on canopy energy budgets and water use efficiency in an irrigated wheat field in the North China Plain. Agric Water Manag 89:116–122
Liu S, Lu L, Mao D, Jia L (2007) Evaluating parameterizations of aerodynamic resistance to heat transfer using field measurements. Hydrol Earth Syst Sci 11:769–783
Liu S, Li SG, Yu GR, Sun XM, Zhang LM, Hu ZM, Li YM, Zhang XZ (2009) Surface energy exchanges above two grassland ecosystems on the Qinghai–Tibetan Plateau. Biogeosci Discuss 6:9161–9193
Makarieva AM, Gorshkov VG (2007) Biotic pump of atmospheric moisture as driver of the hydrological cycle on land. Hydrol Earth Syst Sci 11:1013–1033
Makarieva AM, Gorshkov VG, Li B-L (2013) Revisiting forest impact on atmospheric water vapor transport and precipitation. Theor Appl Climatol 11:79–96. doi:10.1007/s00704-012-0643-9
McNaughton KG, Jarvis PG (1983) Predicting effects of vegetation changes on transpiration and evaporation. In: Kozlowski TT (ed) Water deficit and plant growth, vol 7. Academic Press, New York, pp 1–47
Monteith JL (1981) Evaporation and surface temperature. QJR Meteorol Soc 107:1–27. doi:10.1256/smsqj.45101
Monteith JL, Unsworth MH (1990) Principles of environmental physics. Edward Arnold Press, London

Ochsner TE, Horton R, Ren T (2001) A new perspective on soil thermal properties. Soil Sci Soc Am J 65:1641–1647

Oke TR (1987) Boundary layer climates. Methuen, London

Olejnik JA (1988) The empirical-method of estimating mean daily and mean 10-day values of latent and sensible-heat near the ground. J Appl Meteorol 27:1359–1368. doi:10.1175/1520-0450(1988)-027

Olejnik J, Eulenstein F, Kedziora A, Werner A (2001) Evaluation of a water balance model using data for bare soil and crop surfaces in Middle Europe. Agr Forest Meteorol 106:105–116. doi:10.1016/S0168-1923(00)00208-2

Parker SP (2002) McGraw-Hill Dictionary of scientific and technical terms. 6th edn. McGraw-Hill Professional

Peacock CE, Hess TM (2004) Estimating evapotranspiration from a reed bed using the Bowen-ratio energy balance method. Hydrol Process 18:247–260

Penman HL (1948) Natural evaporation from open water, bare soil, and grass. Proc R Soc Lond 193:120–146. doi:10.1098/rspa.1948.0037

Peters-Lidard CD, Blackburn E, Liang X, Wood EF (1998) The effect of soil thermal conductivity parameterization on surface energy fluxes and temperatures. J Atmos Sci 55:1209–1224. doi:10.1175/1520-0469-(1998)-055

Pielke RA, Avissar R, Raupach M, Dolman AJ, Zeng XB, Denning AS (1998) Interactions between the atmosphere and terrestrial ecosystems: influence on weather and climate. Glob Chang Biol 4:461–475. doi:10.1046/j.1365-2486.1998.t01-1-00176

Pivec J (2002) Analysis of energetic exchange processes within two different forest ecosystems. Ekologia (Bratislava) 21:38–49

Pokorný J, Brom J, Čermák J, Hesslerová P, Huryna H, Nadyezhdina N, Rejšková A (2010) Solar energy dissipation and temperature control by water and plants. Int J Water 5:311–336. doi:10.1504/IJW.2010.038726

Ponting C (1993) A green history of the world. In: The environment and the collapse of great civilizations. Penguin, New York

Powers SM, Johnson RA, Stanley EH (2012) Nutrient retention and the problem of hydrologic disconnection in streams and wetlands. Ecosystems 15:435–449

Rejšková A, Čížkova H, Brom J, Pokorný J (2010) Transpiration, evapotranspiration and energy fluxes in a temperate wetland dominated by *Phalaris arundinacea* under hot summer conditions. Ecohydrology 5:19–27. doi:10.1002/eco.184

Ripl W (2003) Water: the bloodstream of the biosphere. Phil Trans R Soc B 358:1921–1934. doi:10.1098/rstb.2003.1378

Ryszkowski L, Kedziora A (1987) Impact of agricultural landscape structure on energy flow and water cycling. Landsc Ecol 1:85–94

Ryszkowski L, Kedziora A (1995) Modification of the effects of global climate change by plant cover structure in an agricultural landscape. Geographia Polonica 65:5–34

Ryszkowski L, Kedziora A (2007) Modification of water flows and nitrogen fluxes by shelterbelts. Ecol Eng 29:388–400. doi:10.1016/j.ecoleng.2006.09.023

Sanches L, Vourlitis GL, Alves MDC, Pinto-Junior OB, Nogueira JDS (2011) Seasonal pattern of evapotranspiration for a Vochysia divergens forest in Brazilian Pantanal. Wetlands 31:1215–1225. doi:10.1007/s13157-011-0233-0

Schneider ED, Sagan D (2005) Into the Cool: Energy Flow. In: Thermodynamics and Life. University of Chicago Press, Chicago

Schulze E-D, Beck E, Muller-Hohenstein K (2002) Plant ecology. Springer, Berlin

Seják J, Cudlín P, Pokorný J (2012) Valuation ecosystem services as an instrument for implementation of the European landscape convention. In: Westra L, Soskolne C, Spady D (eds) Human health and ecological integrity: ethics, law and human rights. Routledge, New York, pp 69–82

Sikora E, Kossowski J (1993) Thermal conductivity and diffusivity estimations of uncompacted and compacted soils using computing methods. Pol J Soil Sci 26:19–26

Silvan N, Vasander H, Laine J (2004) Vegetation is the main factor in nutrient retention in a constructed wetland buffer zone. Plant Soil 258:179–187

Suleiman A, Crago R (2004) Hourly and daytime evapotranspiration from grassland using radiometric surface temperatures. Agron J 96:384–390

Thom AS (1975) Momentum, mass and heat exchange of plant communities. In: Montheith JL (ed) Vegetation and the atmosphere, vol 1. Academic Press, London, pp 57–110

von Randow C, Manzi AO, Kruijt B, de Oliveira PJ, Zanchi FB, Silva RL, Hodnett MG, Gash JHC, Elders JA, Waterloo MJ, Cardoso FL, Kabat P (2004) Comparative measurements and seasonal variations in energy and carbon exchange over forest and pasture in South West Amazonia. Theor Appl Climatol 78:5–26. doi:10.1007/s00704-004-0041-z

Wallace JS (1995) Calculating evaporation—resistance to factors. Agr Forest Meteorol 73(3–4):353–366

Wang KC, Li ZQ, Cribb M (2006) Estimation of evaporative fraction from a combination of day and night land surface temperature and NDVI. A new method to determine the Priestley–Taylor parameter. Remote Sens Environ 102:293–305. doi:10.1016/j.rse.2006.02.007

Wessel D, Rouse WR (1994) Moisture and temperature limits of the equilibrium evapotranspiration model. J Appl Meteorol 11:436–442

Wever LA, Flanagan LB, Carlson PJ (2002) Seasonal and interannual variation in evapotranspiration, energy balance and surface conductance in northern temperate grassland. Agr Forest Meteorol 112:31–49. doi:10.1016/S0168-1923(02)00041-2

Wierenga PJ, Nielsen DR, Hagan RM (1969) Thermal properties of a soil based upon field and laboratory measurements. Soil Sci Soc Am J 33:354–360

Wilson KB, Baldocchi DD (2000) Seasonal and interannual variability of energy fluxes over a broadleaved temperate deciduous forest in North America. Agr Forest Meteorol 100:1–18. doi:10.1016/S0168-1923(99)00088-X

You ChY, Pence HE, Hasegava PM, Mickelbart MV (2009) Regulation of transpiration to improve crop water use. Crit Rev Plant Sci 28(6):410–431

Zhou L, Zhou G (2009) Measurement and modelling of evapotranspiration over a reed (*Phragmites australis*) marsh in Northeast China. J Hydrol 372:41–47